

Fabrication of encapsulated graphene-based heterostructure using molybdenum as edge-contacts

Illias Klanurak¹, Kenji Watanabe², Takashi Taniguchi³, Sojiphong Chatraphorn¹ and Thiti Taychatanapat^{1*}

¹ Department of Physics, Faculty of Science, Chulalongkorn University, Bangkok 10330, Thailand

² Research Center for Functional Materials, National Institute for Materials Science, Tsukuba, 305-0044 Japan

³ International Center for Materials Nanoarchitectonics, National Institute for Materials Science, Tsukuba, 305-0044 Japan

*Corresponding author's e-mail: thiti.t@chula.ac.th

Abstract. Graphene is an intriguing platform to study exotic quantum transport phenomena due to its intrinsically high mobility and remarkable electronic properties. To achieve high-performance device, graphene is usually encapsulated between thin sheets of hexagonal boron nitride (hBN) to protect graphene layer from extrinsic impurities. Cr/Au is typically employed to make contacts with the edges of the heterostructure. In this research, Mo is used as an alternative electrode for graphene without adhesion layer to simplify the fabrication process. hBN-graphene-hBN heterostructures were fabricated by a pick-up technique and etched in O₂/CHF₃ gases to expose graphene edges. Mo contacts were deposited onto the substrates by sputtering. We achieved ohmic contacts between graphene and Mo. The contact resistance reaches the maximum of around 1,300 Ω·μm at charge neutrality point and decreases to 975 Ω·μm at the density of 4×10¹² cm⁻². We observed that the contact resistance increases over time likely due to the oxidation of Mo but remained ohmic after 2 months. The intrinsic transport characteristics of graphene can still be obtained by using four-probe measurement. Here, we realized a high-quality twisted bilayer graphene device with a room-temperature mobility of 27,000 cm²/V·s indicating that Mo can be used as edge-contacts to probe the transport properties of graphene.

1. Introduction

Two dimensional (2D) materials have gained an enormous interest in the past decade due to their remarkable electrical and mechanical properties. Graphene, a 2D layer of carbon atoms arranged in a honeycomb lattice, is the first 2D material that was extensively studied. In recent years, the observation of superconducting state in twisted bilayer graphene [1] sparks an interest to use a twist angle between layers of graphene or other 2D materials to modify their electronic properties. Nevertheless, to observe exotic phenomena associated with the twist angle, a high-quality graphene device, i.e., a device with low-defect and high-mobility, is a crucial requirement.

hBN is typically used as an insulated substrate for graphene to improve device quality. It can also be used to encapsulate graphene layer, ensuring that extrinsic impurities have neglectable effects on transport properties of graphene. However, the encapsulated structure imposes new limitation for

making electrical contacts between graphene and metal electrodes. One way to overcome this limitation is to expose the edge of graphene by using O_2/CHF_3 plasma to etch the heterostructure. Then, metal electrodes are deposited onto the heterostructure, making one dimensional contact to the edge of graphene [2]. Typically, Au is employed to make electrical contacts with the edges of graphene using Cr as an adhesion layer to improve adhesion between graphene and the metal.

Here, we present Mo as an alternative electrode to make edge-contact with graphene. Mo is selected in this study due to its ability to form covalent bond with carbon atom [3] enabling the realization of the contact without adhesion layer. The carbide formation between Mo and graphene can also enhance orbital overlap at the Mo-C interface which is an important factor for making high quality contact [2].

2. Methods

In this study, we fabricated field-effect transistor (FET) using twisted bilayer graphene (tBLG) as a transport channel and Mo as source-drain electrodes. The tBLG layer was encapsulated between two thin sheets of hBN. Then electrical transport measurement was performed on the device to characterize the quality of graphene and metal contacts.

2.1. hBN-graphene-hBN assembly

Graphene and hBN flakes were obtained by mechanical exfoliation and deposited onto highly doped silicon wafer with thermally-grown SiO_2 . Optical microscope was used to identify usable flakes. Raman spectroscopy was employed to determine the number of graphene layers, and atomic force microscopy was used to determine thickness of hBN flakes. The hBN flakes with thickness of around 10-30 nm were selected to encapsulate graphene layer. The twisted bilayer graphene was created from a single flake of monolayer graphene using tear-and-stack technique [4]. The assembly process was performed under a microscope with a temperature-controlled stage. Here, we used poly(bisphenol A carbonate) film (PC) on a block of Polydimethylsiloxane (PDMS) as a stamp to pick-up top-hBN flake from Si/ SiO_2 substrate. The top-hBN was then used to tear a monolayer graphene flake into two parts: one part remained on Si/ SiO_2 and the other part was picked up with top-hBN. After that, the part of graphene on top hBN was aligned to pick up the part of graphene on Si/ SiO_2 which had been rotated by an angle of $\sim 1.1^\circ$ to form tBLG. The top hBN-tBLG structure was used to pick up bottom-hBN flake, creating hBN-tBLG-hBN heterostructure (BNGBN). All the pick-up process was conducted at $100^\circ C$. In the final step, the heterostructure was slowly released onto another Si/ SiO_2 substrate at stage temperature of $180^\circ C$ to remove contaminants that trapped between interfaces during the assembly process.

2.2. BNGBN characterization

Raman spectroscopy with a laser excitation of 532 nm was employed to characterize the BNGBN. A normalized Raman spectrum of the stacked graphene region is shown in figure 1. We observed a few prominent peaks in the spectral range of $1,100-3,000\text{ cm}^{-1}$. Raman peaks centered at $1,365\text{ cm}^{-1}$ and $1,582\text{ cm}^{-1}$ are characteristic of in-plane vibration of hBN and graphene respectively [5]. The lack of D-peak in the Raman spectrum indicates that the graphene layers are defect-free [6]. To confirm small twist angle between two graphene layers, we investigate 2D peak of graphene at $2,700\text{ cm}^{-1}$ since this peak is sensitive to electronic band structure of graphene. We found that the shape of 2D peak is significantly different than that of Bernal-stacked bilayer graphene as shown in figure 1(b). This implies that our tBLG still retains its twisted angle even after heated at $180^\circ C$ in the layer assembly process.

2.3. Mo contact

To make electrical contacts with the edges of graphene, a rectangular shaped Poly(methyl methacrylate) (PMMA) etch-mask was defined on the BNGBN using electron-beam lithography (EBL). The region of the BNGBN outside of the mask was then etched away by O_2/CHF_3 plasma to expose the edge of graphene. Contacts were defined by EBL followed by DC sputtering of 80 nm-thick Mo film onto the substrate. The deposition process was performed in a high vacuum chamber with a base pressure of 9.6×10^{-7} mbar. Ar gas at a pressure of 6.1×10^{-3} mbar was used as sputtering gas at 550 W. After lift-off process, we obtained tBLG FET device with Mo electrodes as shown in figure 2(a, b).

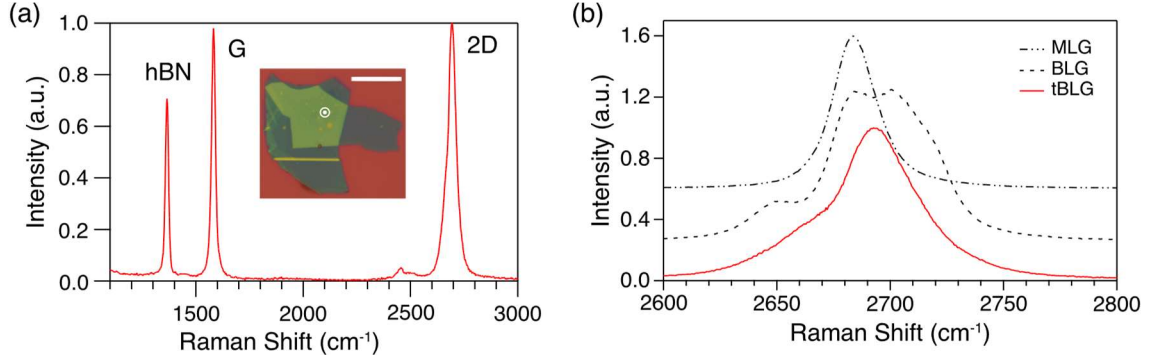


Figure 1. Raman spectrum of the BNGBN using 532 nm laser excitation. (a) Raman spectrum in the spectral range of 1,100-3,000 cm^{-1} and (b) Comparison between Raman 2D peak of graphene for monolayer graphene (MLG), Bernal-stacked bilayer graphene (BLG) and tBLG. The Raman spectra are vertically offset for clarity. The inset shows optical image of the BNGBN on Si/SiO₂ substrate with a circle indicating the position of the laser illuminated on the BNGBN (scale bar is 20 μm).

3. Results and discussion

Electrical transport measurement was performed on the BNGBN at room temperature to characterize the quality of contacts. Inset of figure 2(c) shows the linear behavior between current, I_{SD} , and source-drain voltage, V_{SD} , between contacts 3 and 4 indicating the ohmic contacts between Mo and the edges of graphene. The standard lock-in technique with excitation frequency of 17 Hz was used to measure the transport properties of the BNGBN. Carrier density, n , in graphene channel can be electrically tuned by applying voltage, V_{BG} , to a silicon back-gate. Using parallel plate capacitor model, carrier density in tBLG can be determined by the relation $n = \left(\frac{\epsilon_{r1}\epsilon_{r2}\epsilon_0}{e\epsilon_{r2}d_1 + e\epsilon_{r1}d_2} \right) V_{\text{BG}}$ where e , d_1 , d_2 and ϵ_0 are electron charge, thickness of SiO₂, thickness of hBN and vacuum permittivity, respectively. Here, we used $\epsilon_{r1}=3.7$ and $\epsilon_{r2}=3.2$ for the dielectric constant of SiO₂ and hBN [7].

Figure 2(b) illustrates the measurement setup for measuring contact resistance. First, a bias current, I_{34} , of 100 nA was applied between contacts 3 and 4 and the voltage, V_{34} , across contacts 3 and 4 was measured as a function of V_{BG} . The measured resistance $R_{34}=V_{34}/I_{34}$ can be expressed as $R_{34}=R_{C3}+R_{\text{tBLG}}+R_{C4}$ where R_{tBLG} is a resistance of graphene channel and R_{C_i} is the contact resistance between contact i and graphene. Then, the voltage, V_{14} , across contacts 1 and 4 was measured using the same configuration for current bias. The resistance $R_{14}=V_{14}/I_{34}=R_{\text{tBLG}}+R_{C4}$ was obtained. The contact resistance between contact 3 and graphene as a function of V_{BG} can be extracted by subtracting R_{34} with R_{14} as shown in figure 2(c). We observed that the contact resistance depends on carrier density in tBLG channel. The contact resistance reaches the maximum value of 1,300 $\Omega \cdot \mu\text{m}$ at charge neutrality point (CNP) and decreases to 975 $\Omega \cdot \mu\text{m}$ at 60 V away from CNP which corresponds to carrier density of $\sim 4 \times 10^{12} \text{ cm}^{-2}$. This result is comparable to BN/monolayer graphene/BN devices fabricated by using Cr/Au as edge contacts [2] whose contact resistance varies between 200-2,000 $\Omega \cdot \mu\text{m}$ over similar range of carrier density. To confirm the reproducibility of ohmic contact between Mo and graphene, we fabricated another FET device with Mo edge contacts. We observed that all of 6 contacts in our experiment exhibit ohmic behavior. This indicates that Mo can be used to make reliable contact to the edge of graphene.

We also noticed the change in contact resistance when measuring it again after 57 days as can be seen in figure 2(d). We observed two-fold increase in maximum contact resistance near CNP and asymmetry in the contact resistance around CNP when the charge carrier changes between electron and hole. The contact resistance for electron is larger than hole at the same carrier density. This asymmetry imitates behavior of contact resistance of high work function metal like Pd or Au which is inconsistent with the low work function of Mo [8]. We argue that this asymmetry may be the result of the oxidation of Mo contacts into MoO_x. The large difference in work function between graphene (~ 4.5 eV) and MoO_x

(~ 6.8 eV for MoO_3) causes charge transfer at the contact interfaces resulting in hole doped region at the vicinity of the contacts [3]. The p-doping of tBLG near the contacts acts as p-n junction leading to high contact resistance when the charge carrier is electron. Nevertheless, the contacts between Mo and tBLG still exhibit ohmic behavior as can be seen in the inset of figure 2(d).

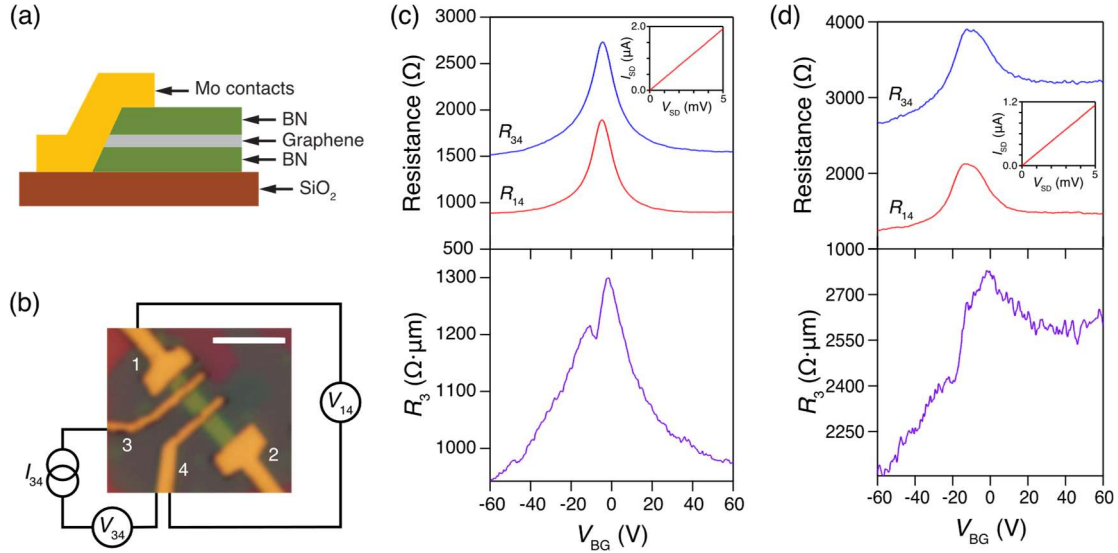


Figure 2. (a) Schematic diagram illustrating cross-section view of the tBLG FET device with Mo edge contacts, (b) diagram of measurement setup for probing contact resistance between Mo and tBLG where each contact is labelled with number 1-4 (scale bar is $5 \mu\text{m}$), (c) measured resistance R_{14} and R_{34} as a function of V_{BG} obtained after the device fabrication along with R_3 calculated by subtracting R_{34} with R_{14} and multiplying the result with the length of 1D contact and (d) contact resistance R_3 obtained after 57 days from the first measurement. Insets in (c) and (d) show ohmic behavior between contacts 3 and 4 of the device measured without applying voltage to the back-gate.

Despite the increase in contact resistance of Mo, the intrinsic transport properties of BNGBN can still be obtained by using four-probe measurement to eliminate the effects of contacts. The CNP was located near the zero back-gate voltage when measure immediately after the fabrication process. However, after 3 months, the CNP was shifted to $V_{BG} \sim -16$ V (see figure 3(a)). Even though the tBLG is encapsulated by hBN, it is possible that dangling σ -bonds at the exposed edges of graphene may react with ambient contamination in air leading to H-terminated edge. The H-terminated edges of tBLG induce n-doping to graphene sheet resulting in the negative shift of CNP [9]. Even after such doping, the device still exhibits a very small hysteresis during sweeping V_{BG} forward and backward as a result of encapsulated structure as shown in figure 3(a). Mobility, μ , of the device is calculated from the slope of conductivity, σ , using Drude model, $\mu = \frac{1}{e} \frac{\partial \sigma}{\partial n}$, as shown in figure 3(c). The room-temperature mobilities of electron and hole reach the values as high as $27,000$ and $21,000 \text{ cm}^2/\text{V}\cdot\text{s}$ at electron and hole density of $5 \times 10^{11} \text{ cm}^{-2}$ and $-4 \times 10^{11} \text{ cm}^{-2}$, respectively. The mobilities in our device are comparable to the state-of-the-art, encapsulated monolayer graphene devices which have room-temperature mobility of $\sim 40,000 \text{ cm}^2/\text{V}\cdot\text{s}$ [2]. This indicates that Mo contacts do not hinder the quality of the graphene and can be employed to study its intrinsic electronic transport properties. Contrary to Bernal-stacked bilayer graphene, we observed non-monotonic behavior in conductivity when V_{BG} was higher than 20 V, shown in figure 3(c). We argued that this may result from the emergence of a new Dirac cone in the electronic band structure at high energy, which is a phenomenon that typically observed in small twist angle bilayer graphene [1].

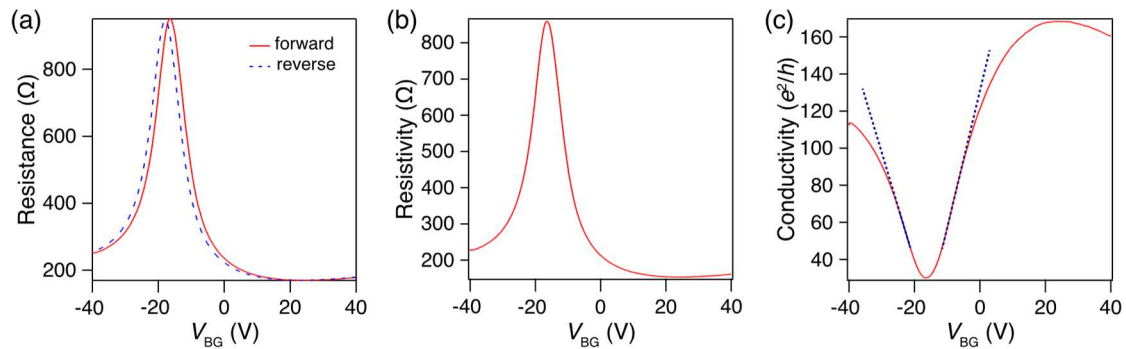


Figure 3. (a) Dirac peak of tBLG obtained from four-probe measurement after 3 months by sweeping V_{BG} forward (solid line) and backward (dash line), (b) resistivity and (c) conductivity extracted from the Dirac peak. The dash lines in figure 3(c) show the slope of conductivity used for calculating electron and hole mobilities.

4. Conclusion

In this work, FET based on hBN-encapsulated tBLG was fabricated using Mo as edge contacts. We realized Ohmic contacts between Mo and tBLG. Despite the increase in contact resistance overtime, it still remains Ohmic and four-probe measurement can still be used to obtain intrinsic electrical properties of graphene. The high mobility at room-temperature indicates that Mo has negligible effect to carrier transport in FET channel. These results demonstrate that Mo can be used as an alternative metal to probe intrinsic characteristics of graphene.

Acknowledgments

This work was supported by the Research Fund for DPST graduate with First Placement (Grant no. 002/2015) and Ratchadaphiseksomphot Endowment Fund of Chulalongkorn University, Grant for Research. I.K. would like to acknowledge the Development and Promotion of Science and Technology Talents Project (DPST) scholarship. The authors would also like to thank K. Jaruwongrunsee (NECTEC, Thailand), B. Namnuan, and P. Panchawirat (ThEP Center, Thailand) and for help with wire bonder, sputtering and E-beam lithography respectively.

References

- [1] Cao Y, Fatemi V, Fang S, Watanabe K, Taniguchi T, Kaxiras E and Jarillo-Herrero P 2018 *Nature* **556** 43–50
- [2] Wang L *et al.* 2013 *Science* **342** 614–7
- [3] Zhang Y and Qu X-P 2019 *AIP Adv.* **9** 055221
- [4] Kim K *et al.* 2016 *Nano Lett.* **16** 1989–95
- [5] Cuscó R, Gil B, Cassabois G and Artús L 2016 *Phys. Rev. B* **94** 155435
- [6] Ferrari A C and Basko D M 2013 *Nat. Nanotechnol.* **8** 235–46
- [7] Campos L C, Young A F, Surakitbovorn K, Watanabe K, Taniguchi T and Jarillo-Herrero P 2012 *Nat. Commun.* **3** 1239
- [8] Xia F, Perebeinos V, Lin Y M, Wu Y and Avouris P 2011 *Nat. Nanotechnol.* **6** 179–84
- [9] Brenner K, Yang Y and Murali R 2012 *Carbon* **50** 637–45